

N64-28970

(ACCESSION NUMBER)

21

(PAGES)

NASA CR 58674

(NASA CR OR TMX OR AD NUMBER)

(THRU)

1

(CODE)

08

(CATEGORY)

Technical Report No. 32-653

*The Design of a Very High Power, Very Low Noise
Cassegrain Feed System for a Planetary Radar*

Philip D. Potter

OTS PRICE

XEROX

MICROFILM

\$

\$

260 ph.

jpl


JET PROPULSION LABORATORY
CALIFORNIA INSTITUTE OF TECHNOLOGY
PASADENA, CALIFORNIA

August 24, 1964

Technical Report No. 32-653

*The Design of a Very High Power, Very Low Noise
Cassegrain Feed System for a Planetary Radar*

Philip D. Potter

A handwritten signature in dark ink, appearing to read "R. Stevens", is positioned above a horizontal line.

Robertson Stevens, Chief Communications
Element Research

JET PROPULSION LABORATORY
CALIFORNIA INSTITUTE OF TECHNOLOGY
PASADENA, CALIFORNIA

August 24, 1964

Copyright © 1964
Jet Propulsion Laboratory
California Institute of Technology

Prepared Under Contract No. NAS 7-100
National Aeronautics & Space Administration

CONTENTS

I. Introduction	1
II. Previous Applicable Cassegrain Work	3
III. Feed System Configuration	4
IV. Microwave Component Design	6
V. Gain and Noise Temperature Performance	9
VI. Performance Analysis and the Possibility of Future Improvement	11
VII. Conclusions	14
References	14

TABLES

1. Antenna gain calibration errors	9
2. Predicted and measured gain and aperture efficiency	12
3. Predicted and measured zenith noise temperature	13

FIGURES

1. Ideal feed patterns	2
2. Cassegrain antenna	2
3. Planetary radar feed system	4
4. Planetary radar antenna system	5
5. Support cone equipment layout	5
6. Feedhorn radiation pattern, E-plane	6
7. Feedhorn radiation pattern, H-plane	6
8. Feedhorn radiation pattern, 45° plane	7
9. Feedhorn section after rough machining	7

FIGURES (Cont'd)

10. Feedhorn undergoing test	8
11. High power turnstile junction	8
12. Antenna calibration range	9
13. Block diagram for 85-ft antenna gain test	10
14. Antenna temperature vs. elevation angle	10
15. Feed system radiation pattern	11
16. Aperture blockage effect	12
17. Truss type quadripod	12
18. Calculated secondary pattern 50% opaque	13
19. Calculated secondary pattern 25% opaque	13
20. Measured secondary patterns	13

ABSTRACT

28970

A modified Cassegrain feed for an 85-ft diameter antenna, planetary radar system is described. The equipment and techniques involved are being developed for use in the National Aeronautics and Space Administration/Jet Propulsion Laboratory Deep Space Instrumentation Facility. The radar system operates at a frequency of 2400 Mc in a duplex mode with a transmitter power of 100 kw CW and an overall receiving system noise temperature of about 28° K. The feed system utilizes a nonoptical subreflector and a suppressed sidelobe feedhorn to achieve an overall aperture efficiency of 0.65 and a zenith antenna noise temperature of 10° K, including atmospheric effects. A versatile polarizing system provides for either sense of circular polarization or for any orientation of linear polarization. Detailed design and performance information is presented.

Author

I. INTRODUCTION

The development of equipments and techniques for the National Aeronautical and Space Administration (NASA)/Jet Propulsion Laboratory (JPL) Deep Space Instrumentation Facility (DSIF) has been aided by the projects performed with an experimental planetary radar system which involved most of the equipments and techniques required to operate a deep space communications station. Large, efficient, low noise antennas are particularly common to both technologies.

The capability of a radar system is directly proportional to the square of the antenna gain and inversely proportional to the receiving system noise temperature; thus, the antenna gain should be maximized and the antenna effective noise temperature minimized. At one time (Ref 1) it was believed that these two requirements were in conflict; recently, however, it was realized that paraboloidal antenna feed systems can be designed which

tend to satisfy both the gain and the noise temperature requirements simultaneously.

For paraboloidal antenna systems of the 85-ft or larger class, it is readily shown that simple economic considerations dictate the use of a highly specialized, high performance feed system. The following empirical relationship may be used to estimate the structural cost of a large antenna as a function of its diameter:

$$C \approx aD^b \quad (1)$$

where C = antenna cost

D = antenna diameter

a = a constant, dependent on design, required accuracy, place of manufacture, etc.

b = a constant ≈ 2.6

The antenna gain, G , is given by

$$G = \pi^2 \eta \left(\frac{D}{\lambda} \right)^2 \quad (2)$$

where $\pi = 3.1416$

η = aperture efficiency

λ = operating wavelength; assumed to be a constant; fixed by system considerations

By combining Eq. (1) and (2) and taking the total differential of G , it is readily shown that to obtain a specified value of G , the cost value ΔC , of an aperture efficiency increase, $\Delta\eta$, is given by

$$\Delta C \approx \frac{b}{2} \frac{C}{\eta} \Delta\eta \quad (3)$$

For typical values of

$\eta = 0.65$ and $b = 2.6$, the fractional cost is:

$$\frac{\Delta C}{C} = 2\Delta\eta \quad (4)$$

Equation 4 means that a 10% increase of aperture efficiency (from 0.60 to 0.70) provides the performance equivalent of reflector diameter change which would result in a 20% increase in structural cost. Because precision antennas of the 85-ft class generally cost from \$300,000 to \$1,000,000, from an economic standpoint alone, the feed system design is worthy of considerable engineering effort.

Also, the reproduction cost of a high efficiency feed is not much greater than a low efficiency feed once the development work is done. However, the cost of reproducing a large reflector antenna remains by a more fixed amount greater than reproducing a small one. Therefore, economy in duplicating antenna installations also favors appropriate effort on feed system design.

Assuming the paraboloidal reflector surface is sufficiently accurate for the frequency of operation, all techniques for maximizing the aperture efficiency and minimizing noise temperature basically involve control of the reflector illumination function. This in turn requires control of the feed system radiation pattern and possibly control of the feed system support structure design to minimize aperture blockage effects. Figure 1 shows three conceptually possible feed system radiation patterns. Figure 1a is the optimum but physically

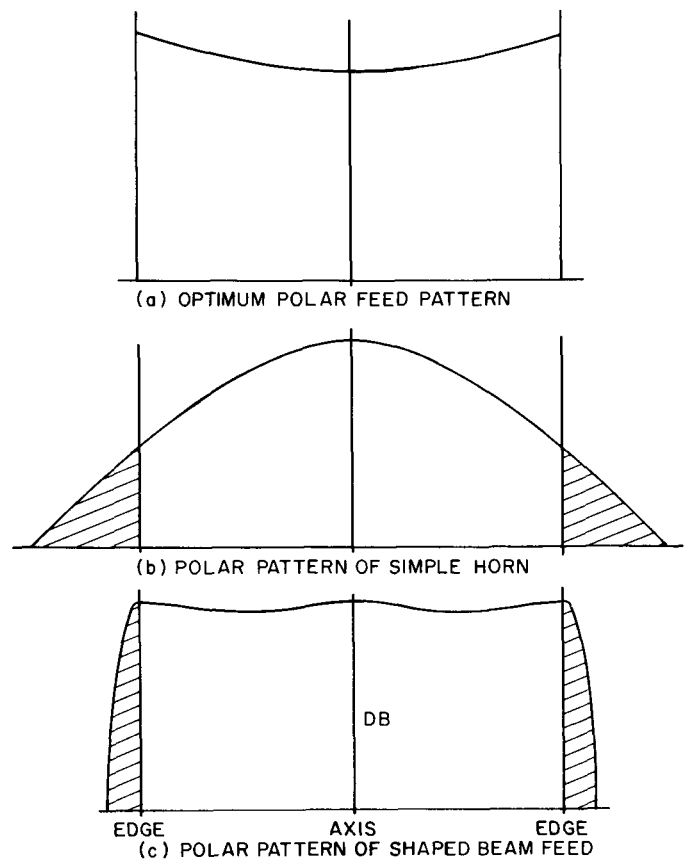


Fig. 1. Ideal feed patterns

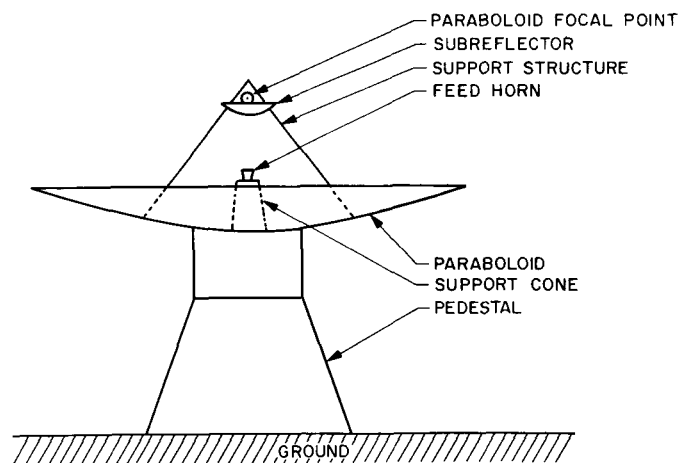


Fig. 2. Cassegrain antenna

unrealizable case where the paraboloid is uniformly illuminated with no spillover, resulting in maximum aperture efficiency (100%) and minimum noise temperature. Figure 1b depicts the type of illumination achieved with a simple horn-type feed. Such a system will typically

have an overall aperture efficiency of 0.50-0.60, spillover of 10-20% and a zenith noise temperature contribution of 20-40° K. Figure 1c is a realizable radiation pattern which will yield a high performance level.

Although performance of the general type depicted in Fig. 1c has been realized in focal point feed systems (Ref. 2), we have found the two reflector Cassegrain-type configuration to be a more practical and operationally convenient approach. The general physical layout of such a system is shown in Fig. 2. A subreflector is interposed between the focal point of the paraboloid and the feed-horn center of radiation which, when viewed as operating in the transmit mode, transforms the feedhorn radiation into a quasi-spherical wave centered at the paraboloid

focal point; in the limit of vanishing wavelength, the subreflector is a truncated hyperboloid. A Cassegrain-type system in which the subreflector shape deviates from a hyperboloid is referred to as nonoptical and generally can be designed to perform superior to a zero wavelength approximation design.

For large ground antennas, the feed support cone may be sizable without significant effect on performance and thus serve as a readily accessible, controlled environment for housing associated RF equipments. For this reason and also because of a high performance potential, JPL chose a modified Cassegrain feed system. Operational experience with the system beginning in October, 1962, has strongly supported this choice.

II. PREVIOUS APPLICABLE CASSEGRAIN WORK

The two-reflector system invented by W. Cassegrain has been used extensively for many years in optical telescopes, primarily to achieve a long effective focal length with a convenient physical configuration. During the last decade, widespread interest has developed in the use of this type of system for microwave frequencies. An excellent tutorial paper on the microwave application was published by Hannan in 1961 (Ref. 3). Hannan discussed the Cassegrain antenna primarily from a geometric optics standpoint and mentioned possible advantages over a focal point feed system: superior physical configuration, greater flexibility in feed system design and possible longer equivalent focal length for simultaneous lobing applications.

The specific advantage of the two-reflector system for applications requiring minimum rear hemisphere radiation and high front-to-back ratio was pointed out by Foldes and Komlos in 1960 (Ref. 4). Detailed experimental measurements are discussed in their paper relating to the deviation of the feed system performance from that which would be expected from one based on geometric optics; their design was, in fact, experimentally optimized taking into account the empirically determined diffraction effects of the optical subreflector. Under JPL sponsorship, this work was extended by Foldes to large

low noise antenna applications (Ref. 5). Almost simultaneously, experimental work at JPL with a low-noise 85-ft diameter Cassegrain system was reported by Potter (Ref. 6). The system described in Ref. 6, designed for use at 960 Mc made use of an empirically-derived non-optical subreflector (Ref. 7) for increased performance; the performance reported was a zenith noise temperature of 9.5° K, including atmospheric and extra atmospheric effects (approximately 3.5° K at 960 Mc), and an aperture efficiency of 0.50.

The microwave performance of a Cassegrain subreflector has been analyzed in detail in a recent paper by Rusch (Ref. 8), who points out that the noise temperature performance of the two-reflector antenna system is primarily a function of the subreflector diffraction characteristics, i.e., its nonoptical behavior. Rusch uses the current distribution method (Ref. 9) of vector diffraction theory to develop a machine program for accurate calculation of the scattering pattern of an optically-designed subreflector, and hence the antenna noise temperature contribution resulting from rearward spillover. This analytical technique has also been extended (Ref. 10) to consider nonoptical subreflectors such as those described in Ref. 7.

Although the zenith noise temperature performance of a Cassegrain antenna is largely a matter of the subreflector design and the wavelength size, the aperture efficiency is primarily a function of the feedhorn design, i.e., the manner in which the subreflector is illuminated. For maximum aperture efficiency, the subreflector should be essentially illuminated uniformly by a feedhorn whose radiation pattern is axially symmetric and cuts off sharply at the subreflector edge. Spillover around the subreflector edge is a serious problem not only because of aperture

efficiency degradation but also because it creates a spurious forward sidelobe level, making the antenna susceptible to solar jamming and increasing the antenna temperature at low elevation angles.

For single frequency channel applications, such as planetary radar studies, the dual mode conical feedhorn (Ref. 11, 12) represents a significant improvement over conventional feedhorns because of its pattern symmetry and low sidelobe level.

III. FEED SYSTEM CONFIGURATION

The antenna performance as a function of the Cassegrain optics configuration was considered previously (Ref. 5, 6) in detail. Within a rather broad range of parameters, aperture efficiency and zenith noise temperature are not particularly sensitive to feedhorn location, subreflector size and other resulting configuration parameters.

The 2400-Mc planetary radar feed system configuration is shown in Fig. 3. Figure 4 is a photograph of the antenna with feed system installed; a second experimental cone is on the ground nearby. The support cone is designed in such a way that it may be mounted or removed from the antenna in 2-4 hr, thereby permitting extensive system checkout of the enclosed receiver and calibration equipment on the ground prior to antenna installation (Fig. 4).

The subreflector of the planetary radar feed system consists of a 96-in.-diameter truncated hyperboloid with a 120-in.-diameter nonoptical beamshaping flange to reduce antenna noise temperature (Ref. 7). Reflection of energy by the subreflector back into the feedhorn, with the attendant impedance mismatch, is prevented by a centrally located vertex matching plate on the subreflector (Ref. 4). The entire subreflector is mounted on a motor driven jackscrew, three-point support system, thereby allowing for remote focussing of the feed system from the control room. Boresight alignment of the antenna is accomplished by manual adjustment of the three jackscrew supports.

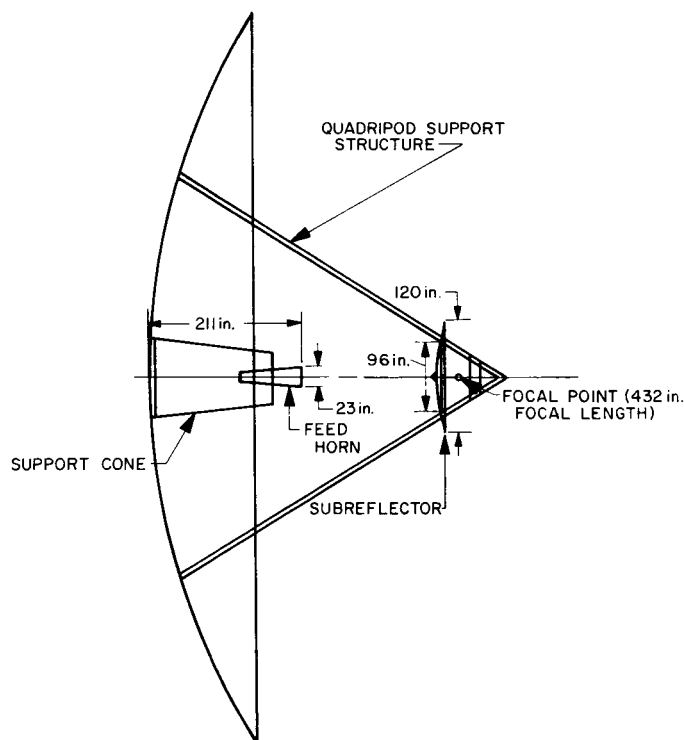


Fig. 3. Planetary radar feed system

A pictorial block diagram of the support cone equipment is shown in Fig. 5. The polarizer is a turnstile junction type (Ref. 13). This type of junction is a six-port device; two ports are spatially orthogonal H_{11} circular waveguide modes, two are H_{10} rectangular waveguide

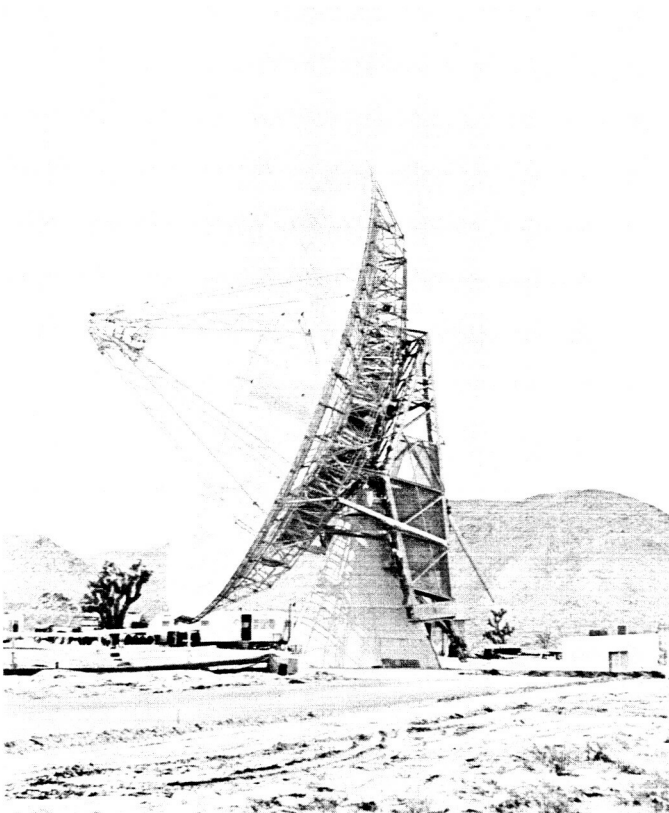


Fig. 4. Planetary radar antenna system

outputs and the final two are short circuit terminated H_{10} rectangular waveguide ports. By appropriate choice of the short circuit lengths, it is possible to excite the feedhorn with any type of polarization. Normally, circular polarization is used for radar experiments; by manual change of the short circuits two continuously rotatable spatially orthogonal modes of linear polarization may be obtained. The polarization switch allows remotely controlled selection of either right- or left-hand circular polarization, or two orthogonal linear polarizations.

As shown in Fig. 5, a second waveguide switch is used to switch the polarizer output either to the high power transmitter or to the receiving system. The third switch allows the receiver (Maser) input to be switched between the antenna or either of two calibrating cryogenic terminations. During the normal transmit mode of

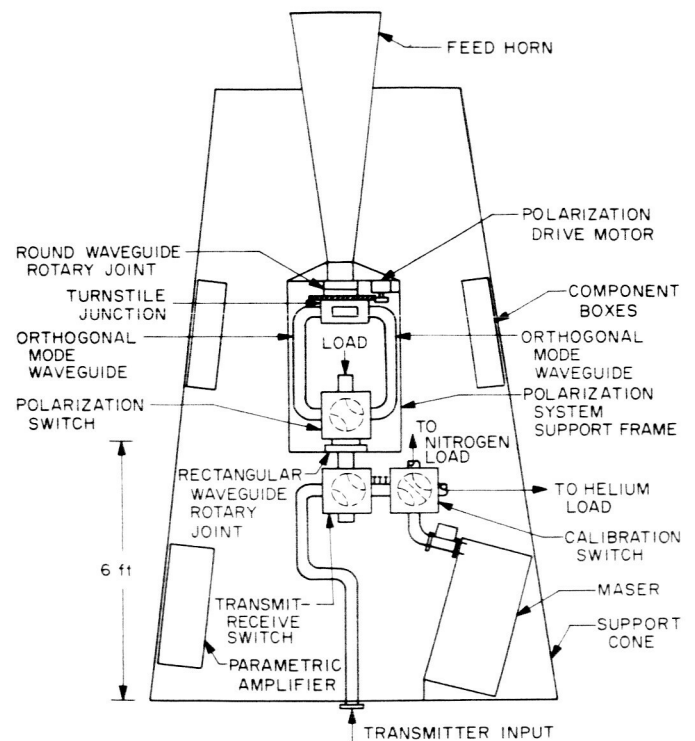


Fig. 5. Support cone equipment layout

radar operation, the polarization switch is in the right circular position, the transmit-receive switch is in the transmit position, and the calibration switch is in the nitrogen load position, the latter to provide additional isolation between transmitter output and receiver input. In the normal receiving configuration, the polarization and transmit-receive switch positions are reversed and the calibrate switch positioned to the antenna port. During radar operation the transmitter drive and switch positions are changed remotely and automatically at time intervals which correspond to the round-trip propagation time between the Earth and the planetary target.

The polarization flexibility and excellent axial ratio of the overall antenna system have been employed by Schuster and Levy (Ref. 14, 15) to perform a number of interesting polarization experiments with the planet Venus as a radar target.

IV. MICROWAVE COMPONENT DESIGN

The feedhorn is a dual mode conical horn (Ref. 11, 12); this type of horn is basically a small flare angle conical horn excited with both the dominant H_{11} and higher-order E_{11} cylindrical waveguide modes, in such a way that the resulting radiation pattern is essentially axially symmetrical, has low sidelobes and negligible cross polarization. The measured feedhorn radiation patterns in the electric, magnetic and diagonal planes are shown in Fig. 6-8 respectively. Because of the desired presence of the higher-order E_{11} mode in the horn, it is necessary to maintain extreme mechanical precision (the order of 10^{-3} wavelength) on the inner surfaces to prevent mode conversion, with attendant pattern degradation. For this reason very conservative mechanical design and fabrication techniques are used; the entire feedhorn was machined from three solid aluminum billets; a typical section is shown in Fig. 9. The completed feedhorn undergoing radiation pattern tests is shown in Fig. 10. It is entirely a figure of revolution, allowing complete polarization flexibility.

The turnstile junction polarizer presented a special problem because of the required high power level (100 kw, CW) during transmit operation. A photograph of the unit is shown in Fig. 11. The cylindrical device protruding from the circular waveguide output is the tuning probe, required for mismatch elimination and port isolation. Between this probe and the circular waveguide wall, TEM coaxial mode energy exists which may cause excessive field strength at the probe surface, with possible arcing. High power tests of the turnstile junction assembly were utilized, in conjunction with conventional microwave measurements, to determine a matching probe configuration which had the desired electrical performance and at the same time would operate at the 100 kw power level. The ellipticity produced by the polarizer, as measured on the entire antenna system, is 0.4 db.

The waveguide rotary joints, switches, bends and other components are of conventional design and do not present any particular problem. All mating flanges were,

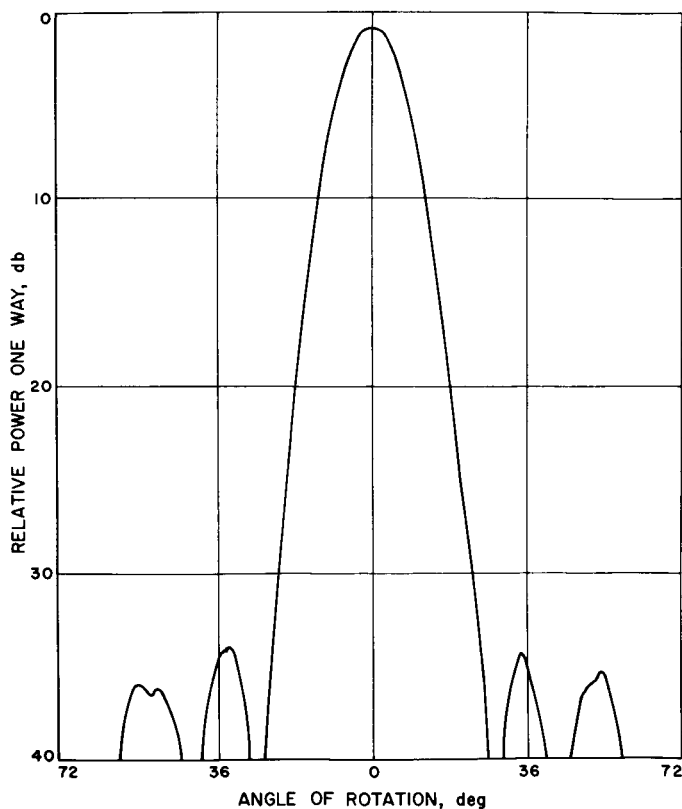


Fig. 6. Feedhorn radiation pattern, E-plane

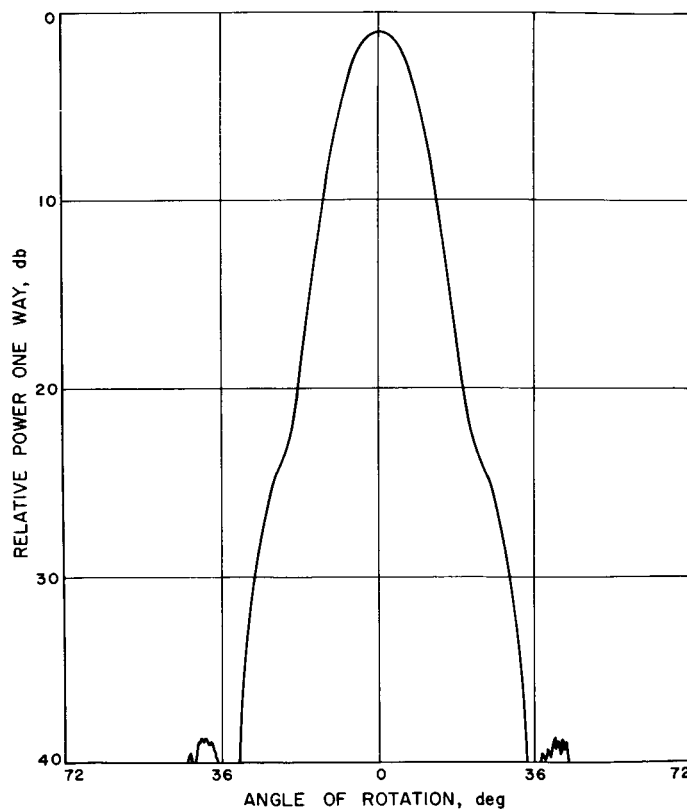


Fig. 7. Feedhorn radiation pattern, H-plane

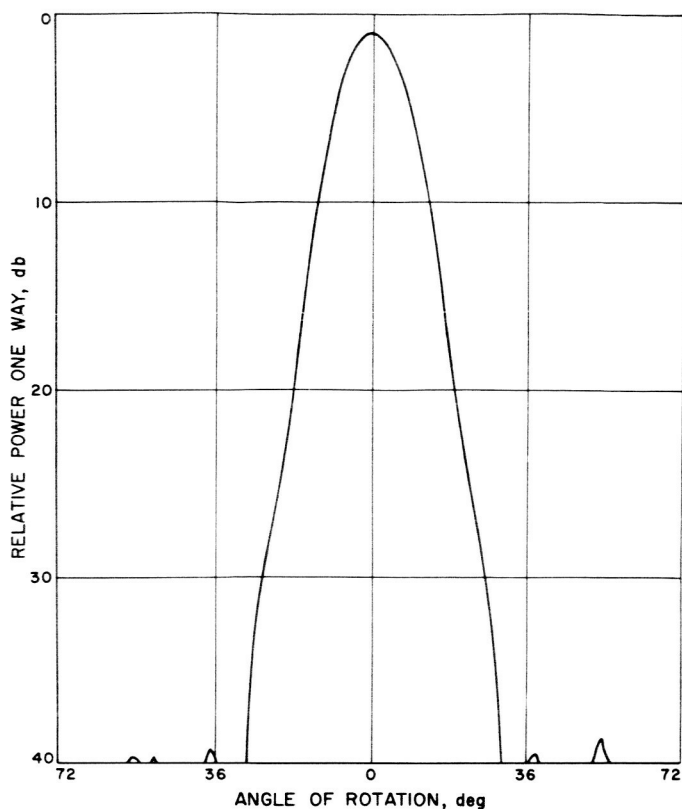


Fig. 8. Feedhorn radiation pattern, 45° plane

however, carefully machined and hand-lapped flat. All components are individually matched to a voltage standing wave ratio of 1.01 to 1.05, and inside surfaces were carefully cleaned to reduce loss and prevent breakdown under power. All high power waveguide parts except the switches and those parts which are in the rotating assem-

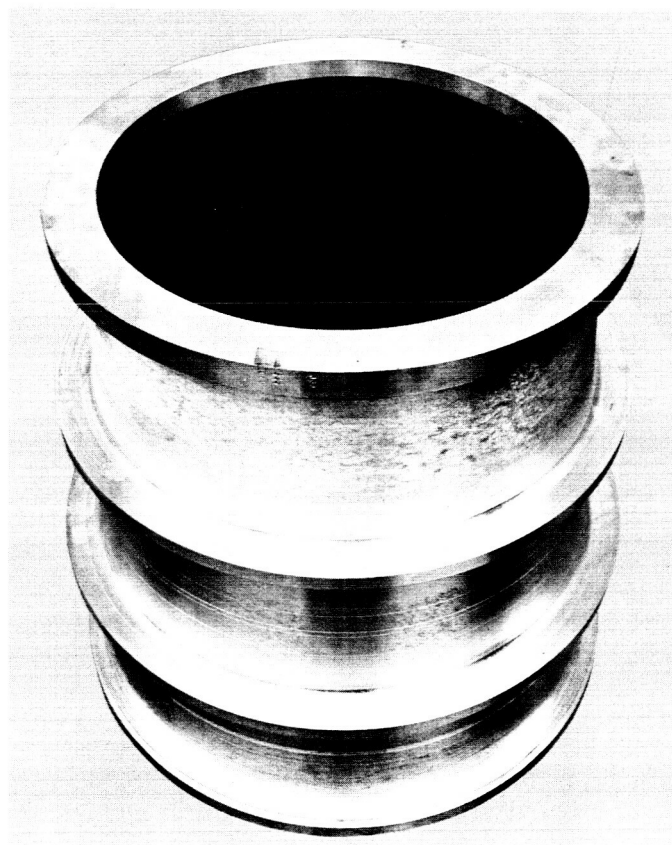


Fig. 9. Feedhorn section after rough machining

bly are water cooled for temperature stability, and the entire waveguide system including the feedhorn is pressurized with dry nitrogen at 0.2 psi above atmospheric pressure to prevent corrosion and to ensure an inert gas for the transmitter tube should its vacuum seal leak.

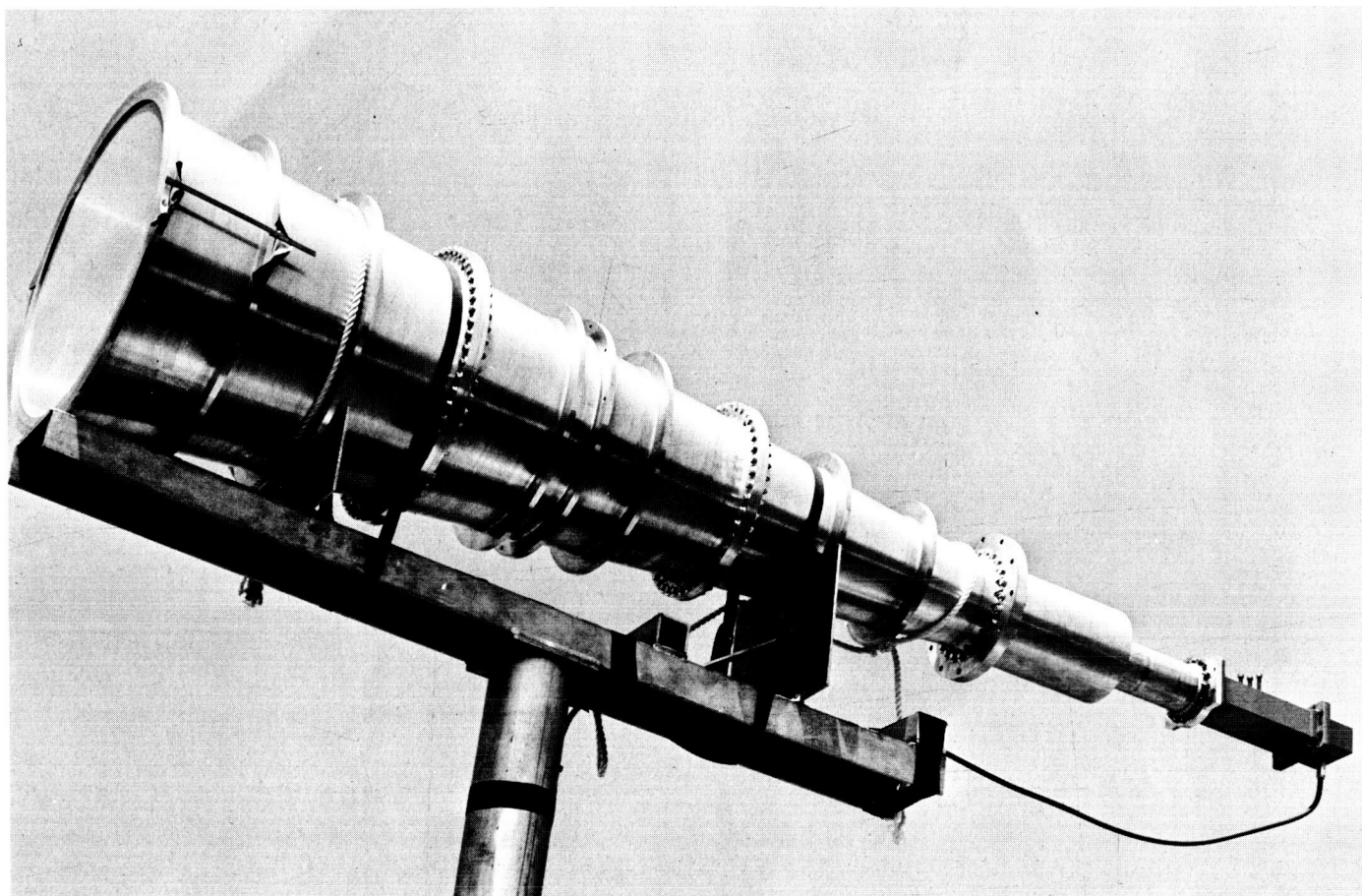


Fig. 10. Feedhorn undergoing test

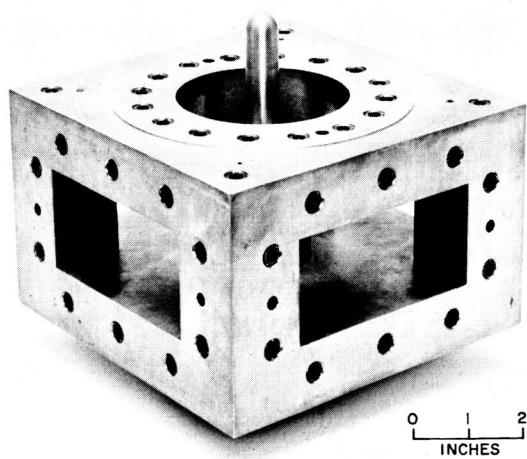


Fig. 11. High power turnstile junction

V. GAIN AND NOISE TEMPERATURE PERFORMANCE

The accurate gain calibration of large antenna systems poses a special problem because of the large distance involved in far field tests. For an 85-ft antenna operating at 2400 Mc the conventional *far-field* distance, i.e., the distance given by twice the ratio of antenna diameter squared to wavelength, is 6.6 statute miles — and an even larger distance is desired for accurate gain calibrations. Consequently, a calibration signal source was installed on Mt. Tiefert, 12.7 mi from the radar antenna. Figure 12 shows the radar installation, Mt. Tiefert and the measurement range.

The technique used for gain calibration involved direct measurement of the signal attenuation between the antenna and the Mt. Tiefert signal source, using suitable corrections for atmospheric loss due to oxygen molecular resonance (Ref. 16, 17). The equipment block diagram for the test is shown in Fig. 13. A total standard deviation of 0.15 db was obtained for the test, as shown in Table 1.

Usually, uncertainty in the standard horn calibration is the most serious error in this type of test. For this reason, a unit identical to the feedhorn was calibrated and used; for the standard gain application, this type of horn has the multiple advantages of: low sidelobes, negligible cross polarized radiation, a well defined phase center close to the aperture, equal beamwidths in all planes, and

Table 1. Antenna gain calibration errors

Error	Estimated standard deviation, db
Standard horn gain	0.09
Signal attenuation	0.05
Multipath	0.05
Coupler calibration	0.05
Atmospheric loss	0.05
Impedance mismatch	0.05
Dissipative losses	0.03
Antenna alignment	0.02
Range length	0.01
Total standard deviation	0.15 db

complete polarization versatility. The horn gain was determined by three independent methods: (1) direct measurement, using a pair of identical units; (2) numerical integration of measured radiation patterns; and (3) analytical integration of the predicted aperture distribution. These three methods yielded 22.17, 21.95 and 21.85 db, respectively. A statistical analysis of these data and the associated errors yields an expected gain value of 22.02 db with a standard deviation of 0.09 db.

Using the above results, the 85-ft antenna gain at the feedhorn output was found to be 54.40 db above isotropic, with a standard deviation of 0.15 db; the corresponding aperture efficiency is 0.65. This measurement

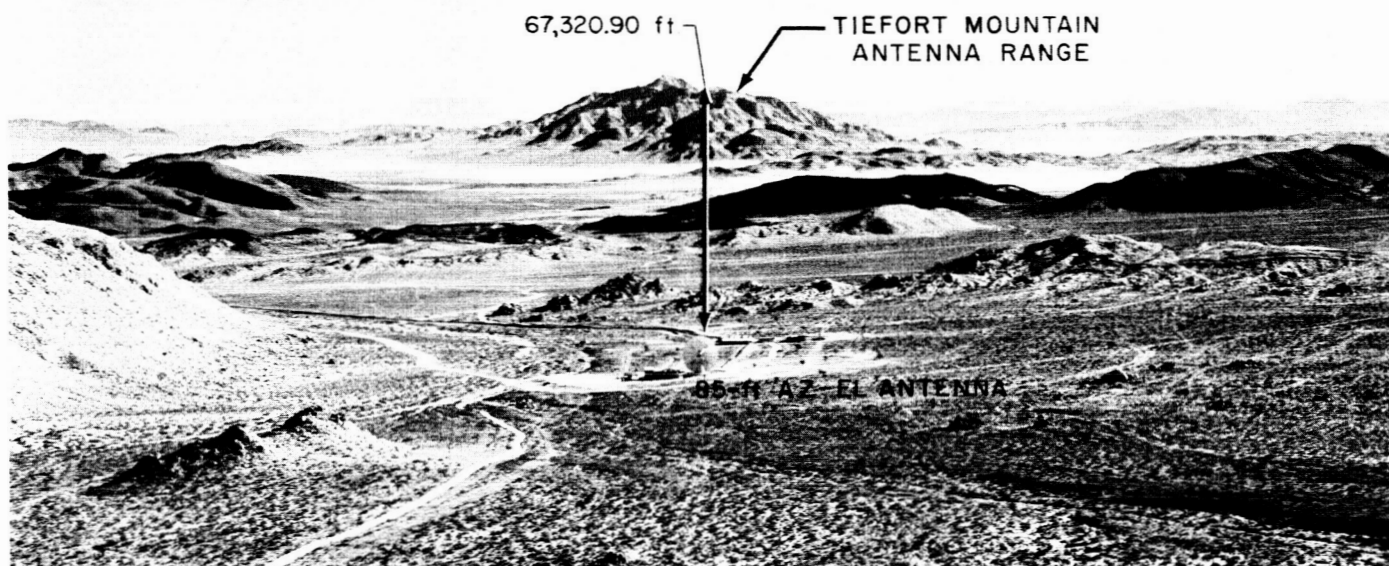


Fig. 12. Antenna calibration range

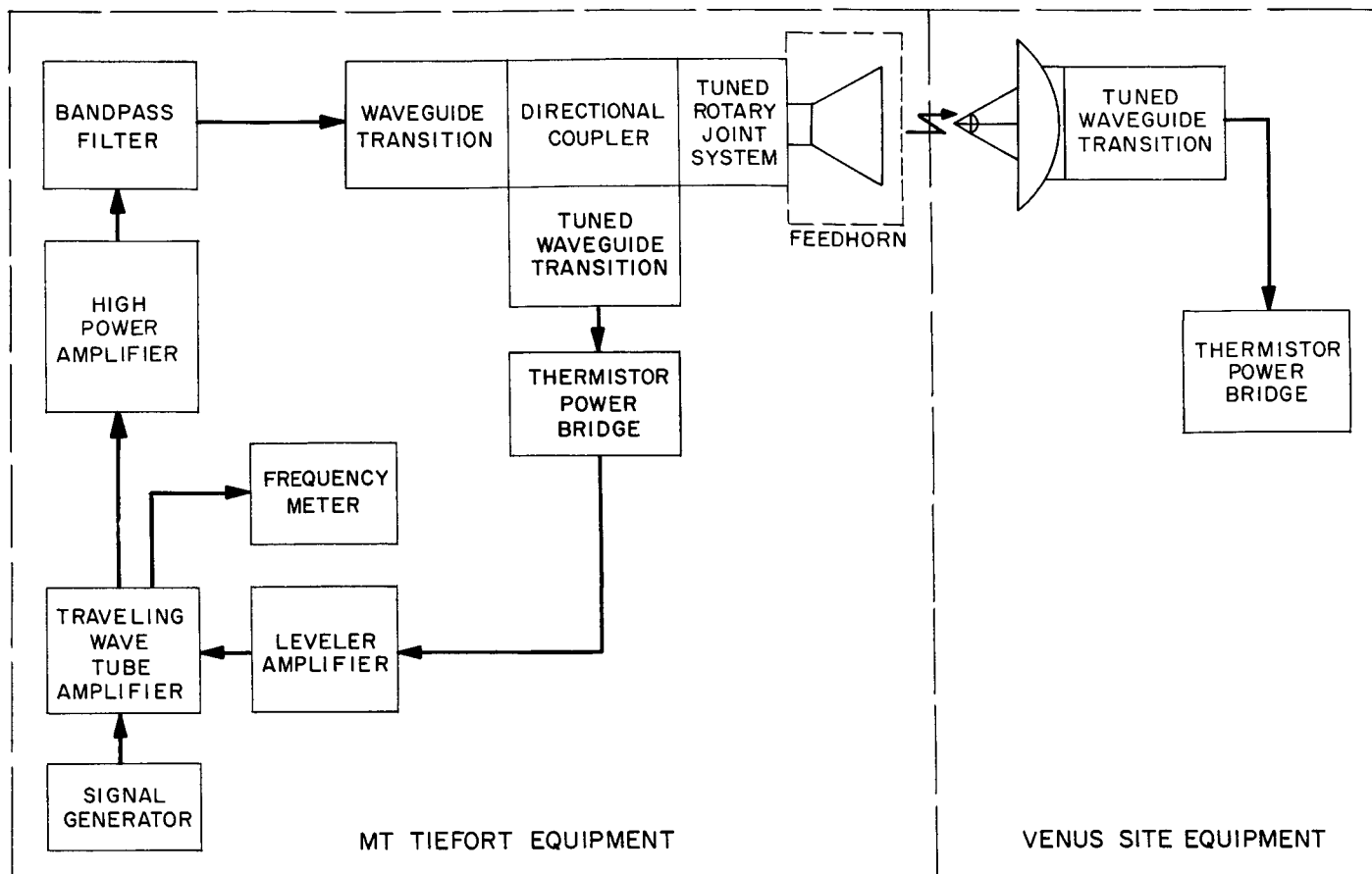


Fig. 13. Block diagram for 85-ft antenna gain test

is believed to be one of the most accurate gain calibrations ever performed of an 85-ft antenna, and it is presently being used (Ref. 18) for calibration of radio source absolute flux density. This work, when completed, will provide a convenient and accurate means of gain evaluation and comparison of the antennas in the NASA/JPL DSIF.

General techniques for determining effective antenna temperature have been derived by Schuster et al (Ref. 2). The method used for evaluating the planetary radar system basically consists of comparing the noise power received by the antenna with that emitted by the liquid nitrogen and liquid helium terminations. Corrections for the small (0.1 db) insertion losses in the various transmission paths were made, resulting in an overall standard deviation for the zenith antenna temperature of approximately 0.75° K. The mean value for the antenna temperature at the feedhorn output is 10.5° K. Figure 14 is a plot of the antenna temperature as a function of elevation angle, together with the temperature which would be observed if the only elevation angle dependence were

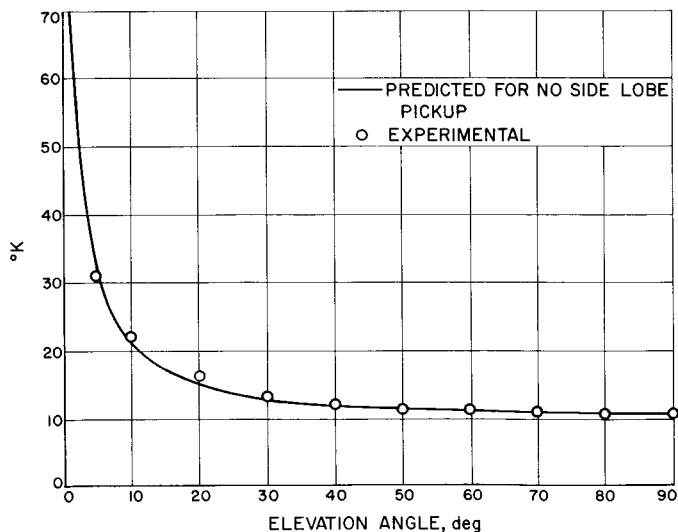


Fig. 14. Antenna temperature vs. elevation angle

that predicted by Hogg (Ref. 17) for the atmosphere. Note that the forward sidelobe contribution to antenna noise temperature is scarcely discernible.

VI. PERFORMANCE ANALYSIS AND THE POSSIBILITY OF FUTURE IMPROVEMENT

The radiation pattern of a paraboloidal antenna may be calculated by integration of its aperture distribution (Ref. 19); the radiation pattern, $g(\theta, \phi)$, is given by

$$g(\theta, \phi) = \int_0^{2\pi} \int_0^a F(\rho, \phi') e^{ik\rho \sin \theta \cos(\phi - \phi')} \rho d\rho d\phi' \quad (5)$$

where

θ = antenna polar pattern angle

ϕ = antenna azimuth pattern angle

k = free space propagation constant

ϕ' = azimuth coordinate of a point in the aperture

ρ = radial coordinate of a point in the aperture

a = aperture radius

$F(\rho, \phi')$ = complex aperture field distribution

Equation (5) is based on scalar diffraction theory and is valid when $F(\rho, \phi')$ is a slowly varying function of posi-

tion and has small phase error, and when θ is much smaller than 90° . $F(\rho, \phi')$ is established by two factors: the feed system radiation pattern and the aperture blockage.

The planetary radar feed system polar radiation pattern, i.e., the pattern of the feedhorn-subreflector combination, is shown in Fig. 15. The relatively uniform radiation in the angular region subtended by the paraboloid ($\pm 60^\circ$) and low rearward spillover are evident. The radiation pattern, experimentally determined by scale model tests and by machine computation (Ref. 10) is essentially axially symmetric, as would be expected from the symmetric feedhorn pattern and subreflector of revolution.

Typical aperture blockage effects are depicted in Fig. 16, which is a nighttime photograph taken of a smaller Cassegrain antenna whose feedhorn had been replaced by a suitable light source. The blockage is of two types: (1) a central circular area caused by the subreflector, and (2) radial wedge-shaped areas caused by the quadri-pod support structure. The physical configuration of the

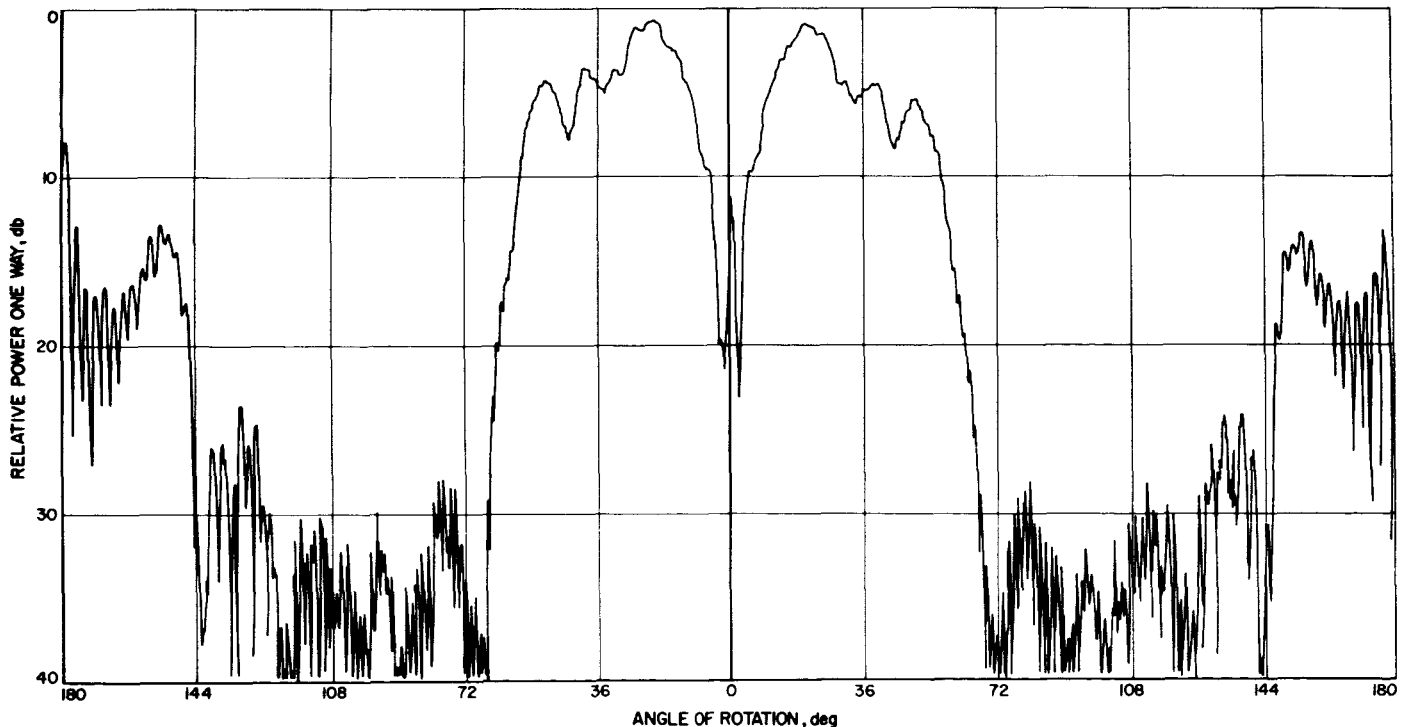


Fig. 15. Feed system radiation pattern

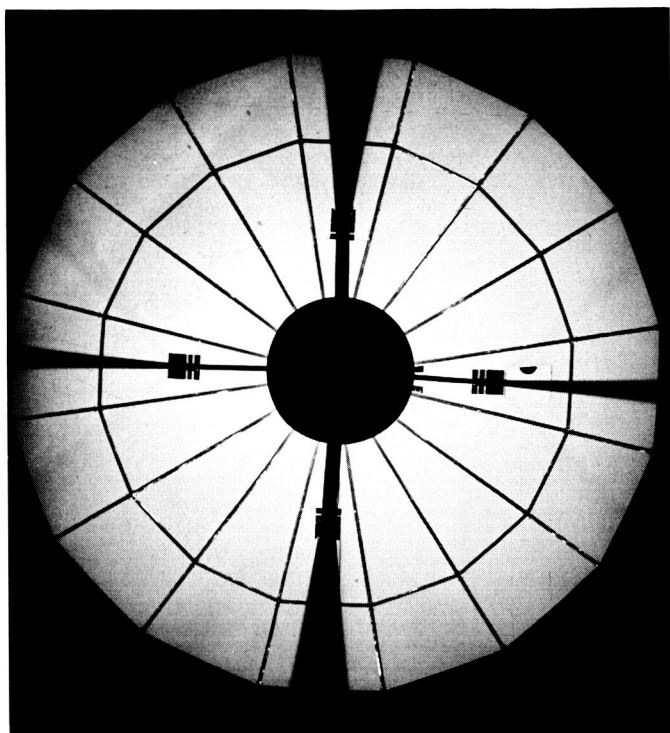


Fig. 16. Aperture blockage effect

quadripod support and the subreflector on the 85-ft radar antenna may be seen in Fig. 17.

A machine program has been developed at JPL for evaluation of Eq. (5), using feed radiation pattern data and calculated aperture blockage. The quadripod is included in the calculation as four wedge-shaped regions, corresponding to the physical outline of the trusswork. An opaqueness factor is introduced in the quadripod-blocked region to account for the fact that the trusswork will, on the average, transmit collimated energy varying from zero (100% opaqueness) to full illumination (0% opaqueness). Figures 18 and 19 are machine computed secondary patterns of the 85-ft antenna for 50 and 75% opaqueness, respectively. The true opaqueness of this quadripod is estimated by a comparison with the experiment radiation patterns shown in Fig. 20. Although there is clearly quadripod polarization dependence, the opaqueness appears to lie between 50 and 75%. From a knowledge of the geometrical outline blockage of the quadripod, which is 14.4%, the quadripod microwave blockage is found to lie between 7 and 11%. The corresponding loss of aperture efficiency due to this effect is -0.6 to -1.0 db. As shown below, a value of -0.73 db (9% blocking) results in perfect agreement between calculated and measured aperture efficiency, and is considered a reasonable estimate of the true effect.

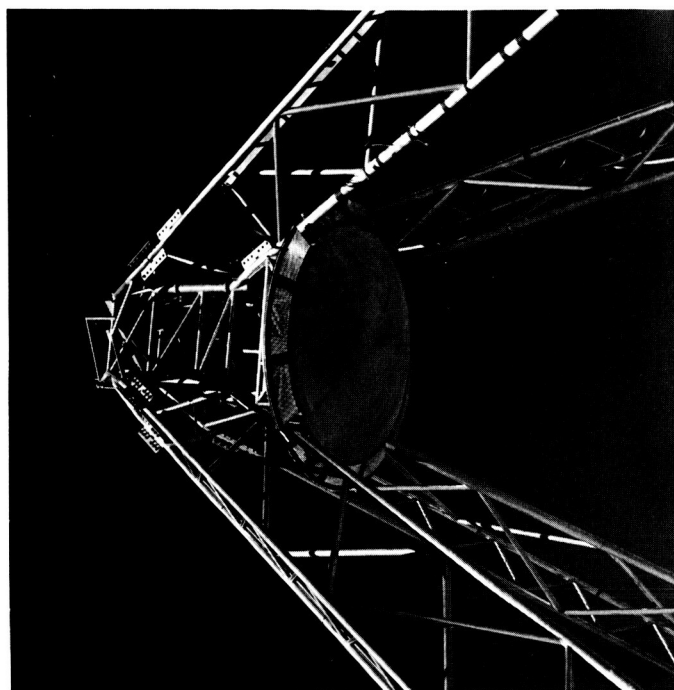


Fig. 17. Truss type quadripod

The predicted (calculated) overall gain and aperture efficiency are compared with the measured values in Table 2.

Table 2. Predicted and measured gain and aperture efficiency

Item	Associated gain, db	Aperture efficiency
Theoretical maximum	56.24	1.000
Illumination factor (includes phase loss)	-1.06	
Gain for perfect surface and no quadripod	+55.18	0.783
Surface tolerance loss (0.032-in. rms)	-0.05	
Gain for no quadripod	+55.13	0.775
Gain loss for 100% opaque quadripod (machine computed)	-1.19	
Gain loss for 63% opaque quadripod	-0.73	
Gain for 63% opaque quadripod	+54.40	0.655
Measured gain	54.40 ± 0.15 standard deviation	0.655 ± 0.020 standard deviation

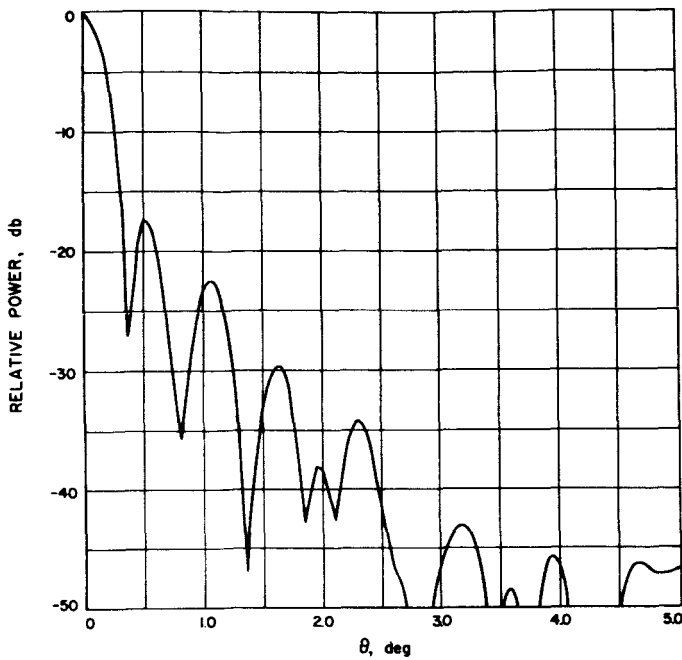


Fig. 18. Calculated secondary pattern 50% opaque

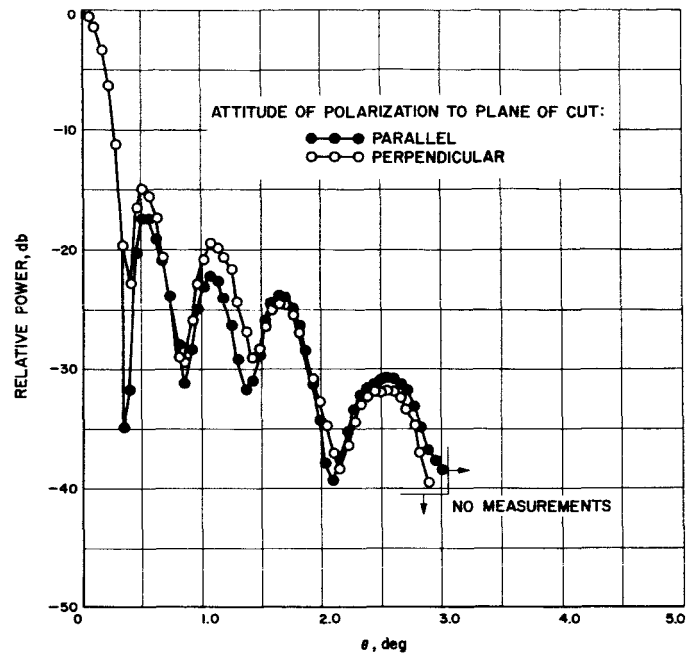


Fig. 20. Measured secondary patterns

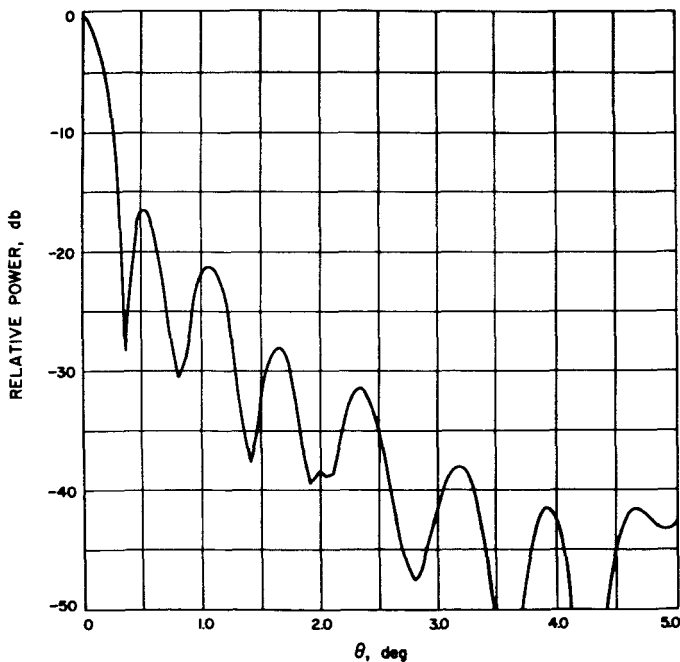


Fig. 19. Calculated secondary pattern 25% opaque

The illumination factor of -1.06 db was calculated by numerical integration (Ref. 20) of the feed system radiation pattern shown in Fig. 15. As mentioned above, there is no significance to the exact value of 63% opaqueness, other than the ensuing agreement between calculated and measured antenna gain. Table 2 not only shows that

antenna gain may be precalculated to good accuracy, but also indicates possibilities for future improvement. Although the illumination loss is only -1 db, it appears, based on present studies in progress at JPL, that further feed system development could effect an improvement of roughly 0.5 db in this area. Similarly, it appears that the effective quadripod blockage could be reduced by more efficient structural design; reduction of this effect to -0.25 db (3% blockage) appears reasonable. An overall improvement of approximately 1 db, therefore, appears possible.

Predicted and measured zenith antenna noise temperature performance is shown in Table 3.

Table 3. Predicted and measured zenith noise temperature

Feed spillover (0.5%)	1.0°K (predicted from scale model tests)
Quadripod scattering	5.5° (predicted from 9% blocking, energy assumed to scatter isotropically, averaged 240°K ground)
Surface leakage between panels	0.5° (extrapolated from a measured value at a different frequency)
Atmosphere and extra atmospheric noise	3.0 (measured)
Predicted total	10.0°K
Measured total	10.5° \pm 0.75 standard deviation

Table 3 demonstrates that zenith noise temperature may be predicted to good accuracy from a knowledge of the feed system patterns and the antenna physical characteristics. Reduction of the quadripod blockage to 3%, as described above, would reduce that contribution to 2° K; also, future feed system improvement to 0.5° spillover contribution appears reasonable. Therefore, it

is felt that a total zenith noise temperature, at S-band frequency, of $6-7^{\circ}$ K is a practical goal for future paraboloidal antenna systems. With no other receiving system improvements, this could reduce the overall system noise temperature from 28 to 24° K, an improvement in sensitivity of 0.7 db. Improvement would, of course, be more dramatic with lower-noise receiving systems.

VII. CONCLUSIONS

A 2400-Mc Cassegrain-type 85-ft-diameter paraboloidal antenna for a planetary radar system has been described. It is applicable in deep space communication systems. It is shown that the performance level is within approximately 2 db of fundamental limits. Based on this

fact, economic considerations, and favorable operational experience over a two-year period, it is believed that a two-reflector paraboloidal antenna is a sound approach to large aperture, low noise applications such as planetary radar.

REFERENCES

1. Cutler, C. C., "Parabolic-Antenna Design for Microwaves," *Proceedings of the IRE*, Vol 35, November, 1947, pp 1284-1294.
2. Schuster, D., et al, "The Determination of Noise Temperature of Large Paraboloidal Antennas," *IRE Transactions on Antennas and Propagation*, Vol AP-10, No. 3, May, 1962, pp 286-291.
3. Hannan, P. W., "Microwave Antennas Derived from the Cassegrain Telescope," *IRE Transactions on Antennas and Propagation*, Vol AP-9, March, 1961, pp 140-153.
4. Foldes, P. and S. G. Komlos, "Theoretical and Experimental Study of Wideband Paraboloid Antenna with Central Reflector Feed," *RCA Review*, Vol XXI, March, 1960, pp 94-116.
5. Foldes, P., "The Capabilities of Cassegrain Microwave Optics Systems for Low Noise Antennas," *Proceedings of the Fifth Agard Avionics Panel Conference*, Oslo, Norway, Vol 4, 1962, Pergamon Press, Ltd., pp 319-352.
6. Potter, P. D., "The Application of the Cassegrain Principle to Ground Antennas for Space Communications," *IRE Transactions on Space Electronics and Telemetry*, Vol SET-8, June, 1962, pp 154-158.

REFERENCES (Cont'd)

7. Potter, P. D., "Unique Feed System Improves Space Antennas," *Electronics*, Vol 35, June 22, 1962, pp 36-40.
8. Rusch, W. V. T., "Scattering from a Hyperboloidal Reflector in a Cassegrainian Feed System," *IEEE Transactions on Antennas and Propagation*, Vol AP-11, No. 4, July, 1963, pp 414-421.
9. Silver, S., "Microwave Antenna Theory and Design," *MIT Radiation Laboratory Series*, Vol 12, McGraw-Hill Book Co., New York, N. Y., 1949, pp 133-150.
10. Rusch, W. V. T., *Scattering of a Spherical Wave by an Arbitrary Truncated Surface of Revolution*, Technical Report No. 32-434, Jet Propulsion Laboratory, Pasadena, May 27, 1963.
11. Potter, P. D., "A New Horn Antenna with Suppressed Sidelobes and Equal Beamwidths," *Microwave Journal*, Vol VI, No. 6, June 1963, pp 71-78.
12. Potter, P. D. and A. C. Ludwig, "Beamshaping by Use of Higher Order Modes in Conical Horns," *Nerem Record*, 1963, pp 92-93.
13. Potter, R. S., *The Analysis and Matching of the Trimode Turnstile Waveguide Junction*, Report No. 4670, Naval Research Laboratory, Washington, D.C., December, 1955.
14. Schuster, D. and G. S. Levy, "Faraday Rotation of Venus Radar Echoes," *Astronomical Journal*, Vol 69, No. 1, February, 1964, pp 42-48.
15. Levy, G. S. and D. Schuster, "Further Venus Radar Depolarization Experiments," *Astronomical Journal*, Vol 69, No. 1, February, 1964, pp 29-33.
16. Van Vleck, J. H., "Absorption of Microwaves by Oxygen," *Physical Review*, Vol 71, No. 6, March 15, 1947, pp 413-433.
17. Hogg, D. C., "Effective Antenna Temperatures due to Oxygen and Water Vapor in the Atmosphere," *Journal of Applied Physics*, Vol 30, No. 9, September, 1959, pp 1417-1419.
18. Levy, G. S., Jet Propulsion Laboratory, Pasadena, California, Private Correspondence.
19. Silver, S., "Microwave Antenna Theory and Design," *MIT Radiation Laboratory Series*, Vol 12, McGraw-Hill Book Co., New York, N. Y., p 192.
20. Potter, P. D., "Aperture Illumination and Gain of a Cassegrainian System," *IEEE Transactions on Antennas and Propagation*, Vol AP-11, No. 3, May, 1963, pp 373-375.

ACKNOWLEDGMENT

This Report is the result of the efforts of numerous individuals at JPL. The application of the Cassegrain principle to large, low noise antennas was first suggested to the JPL antenna staff by E. Rechtin. The planetary radar project was conceived, designed and supported by W. K. Victor and R. Stevens. The author is also indebted to the latter for his continuing interest in and support of low-noise systems, particularly antenna feed systems. The polarization system was conceived, designed and tested by G. S. Levy, R. Petrie and the late Danver Schuster, who also participated with the author in many stimulating feed system design discussions. The author is also indebted to D. Nixon and F. McCrea for their assistance in the installation and testing of the system, and to D. Bathker for his calculation of the secondary patterns.